

DEVELOPMENT AND PERSISTENCE OF HAZARDOUS ATMOSPHERES IN A GLACIOVOLCANIC CAVE SYSTEM—MOUNT RAINIER, WASHINGTON, USA

Christian Stenner^{1, c}, Andreas Pflitsch², Lee J. Florea³, Kathleen Graham¹, and Eduardo Cartaya⁴

Abstract

Glaciovolcanic cave systems, including fumarolic ice caves, can present variable atmospheric hazards. The twin summit craters of Mount Rainier, Washington, USA, host the largest fumarolic ice cave system in the world. The proximity of fumarole emissions in these caves to thousands of mountaineers each year can be hazardous. Herein we present the first assessment and mapping of the atmospheric hazards in the Mount Rainier caves along with a discussion on the microclimates involved in hazard formation and persistence. Our results are compared to applicable life-safety standards for gas exposure in ambient air. We also describe unique usage of Self-Contained Breathing Apparatus (SCBA) at high altitude. In both craters, subglacial CO₂ traps persist in multiple locations due to fumarole output, limited ventilation, and cave morphology. CO₂ concentrations, calculated from O₂ depletion, reached maximum values of 10.3 % and 24.8 % in the East and West Crater Caves, respectively. The subglacial CO₂ lake in West Crater Cave was persistent, with atmospheric pressure as the main factor influencing CO₂ concentrations. O₂ displacement exacerbated by low O₂ partial pressure at the high summit altitude revealed additional cave passages that can be of immediate danger to life and health (IDLH), with O₂ partial pressures as low as 68.3 mmHg. Planning for volcanic research or rescue in or around similar cave systems can be assisted by considering the implications of atmospheric hazards. These findings highlight the formation mechanisms of hazardous atmospheres, exploration challenges, the need for mountaineering and public awareness, and the broader implications to volcanic hazard assessment and research in these environments.

INTRODUCTION

Mount Rainier is an iconic landmark in the U.S. Pacific Northwest. Designated as a Decade Volcano by the International Association of Volcanology and Chemistry of the Earth's Interior (IAVCEI), the U.S. Geological Survey lists Mount Rainier as the third highest volcanic threat in the United States and a 'very high threat' category location in the National Volcanic Early Warning System (Ewert et al., 2018). A popular mountaineering objective, Mount Rainier National Park reports that approximately 10,500 people attempt to climb Mount Rainier each year (NPS, 2020). The National Research Council (1994) has identified the need for monitoring of hydrothermal activity, including fumaroles in the summit area, and changes in surface appearance, such as distribution of snow and ice cover.

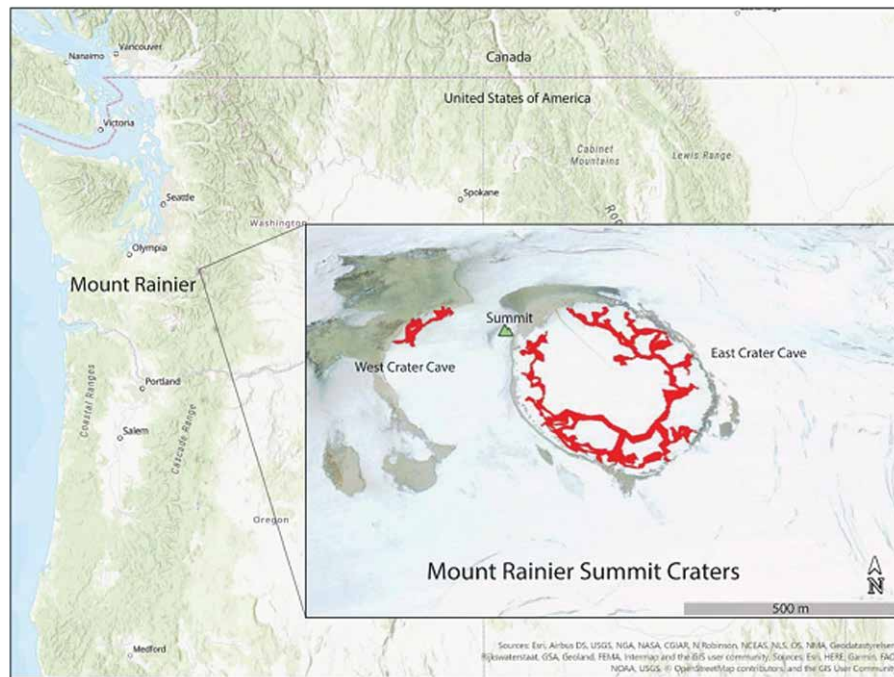


Figure 1. Base map of the Pacific Northwest, United States of America, with the location of Mount Rainier. Inset image of the surveyed extent of the East and West Crater cave system passages at the summit of Mount Rainier, marked in red and overlaid on GIS satellite.

The world's largest fumarolic ice caves exist underneath the glaciers in the summit craters (Fig. 1). They were formed by >100 fumaroles and include a network of 3.5 km of subglacial passages in the East Crater (Florea et al., 2021). A further 300 m of passages exist in the more volcanically active West Crater Cave (Fig. 1). Previous studies in the caves attempted to understand their morphology and the hydrothermal activity (Kiver and Steele, 1975; Frank, 1995; Zimelman et al., 2000). Addi-

¹ Alberta Speleological Society, Calgary, Alberta, Canada

² Department of Geography, Ruhr-University Bochum, Bochum, 44801, Germany

³ Washington State Geological Survey, Department of Natural Resources, Olympia, Washington, USA

⁴ Glacier Cave Explorers, Oregon High Desert Grotto of the National Speleological Society, Redmond, Oregon, USA

^cCorresponding author: (cstenner@telus.net)

tionally, the characteristics of these unique subglacial environments are thought to mimic void spaces in ice masses in other parts of the solar system (Curtis 2016, 2020). The National Academies of Sciences, Engineering, and Medicine (2019) report on astrobiology highlighted the importance of understanding terrestrial subsurface sites as crucial to the search for life on other worlds. Fumarolic ice caves are dark, oligotrophic volcanic environments that may provide insight into microbial communities as an analog for icy conditions such as those which exist on other worlds (Tebo et al., 2015; Davis et al. 2020). As Mars' lower atmosphere consists of 95.32 % CO₂ (Owen et al., 1977), a low atmospheric air pressure and high CO₂, the glaciovolcanic cave setting could be a particularly intriguing Mars polar analog.

Volcanic areas host harmful gasses such as H₂S, SO₂, CO₂, CO, and others (e.g., Hansell and Oppenheimer, 2005; Williams-Jones and Rymer, 2014). Williams-Jones and Rymer (2014) noted the importance of monitoring of gas and public education as the most effective means of hazard reduction. CO₂ can be released by volcanic systems during noneruptive periods and is often disregarded (D'Alessandro, 2006; Williams-Jones and Rymer, 2014). On review of volcanic gas fatalities, D'Alessandro (2006) concluded that CO₂ is the most dangerous volcanic gas, responsible for 90 % of victims. CO₂ is considered to be an immediate danger to life and health (IDLH) at 40,000 ppm (4 %) and can result in unconsciousness after one minute of exposure at greater than 11 % (CDC, 1994a; Williams-Jones and Rymer, 2014). For SO₂ and H₂S, levels above 100 ppm are considered IDLH (CDC, 1994b; 1994c). H₂S exposure can result in eye, nose, throat, and lung irritation at low levels (20–50 ppm) and unconsciousness and death at 500–700 ppm (Enform, 2013). SO₂ exposure ranges from low levels causing sneezing and coughing at 10 ppm, and bronchospasm at 20 ppm, but higher or longer exposures can cause death from airway obstruction (ATSDR, n.d.). These impacts affect safety in fumarolic areas and fumarolic ice caves. On Mount Hood, a well-known fumarole cave was the subject of multiple climbing accidents when a climber slid into the cave where gasses vent (KGW Staff, 2014; Young, 2015). Mammoth Mountain Fumarole in California caused the death of three persons who may have been unaware of the dangers of fumarole gasses (Cantrell and Young, 2009). In the cases of these fatalities, two initial victims fell into the hazardous atmosphere, and two rescuers lost consciousness. Only one of those rescuers survived and multiple rescuers experienced symptoms (Cantrell and Young, 2009). These incidents demonstrate the cascading effect of a single casualty in hazardous atmospheres, whereby responders to the initial victim also succumb to the toxic atmosphere, multiplying the casualties.

O₂ displacement by other gasses has discreet hazards. For example, a climber suffocated in the O₂-poor environment of Mount Hood ice caves in 1934 (Anderson, n.d.). The report identified difficulties in the rescue/recovery whereby rescuers were overcome with fumes and a filter mask did not assist. O₂ helmets were eventually worn by rescuers to complete the recovery. As tissues fail to receive necessary O₂ in environments of 94 mmHg of partial O₂ pressure (PO₂), symptomatic response can develop rapidly (Rom, 1992) including excessive rate and depth of breathing at rest (hyperventilation), poor judgment and coordination, and tunnel vision. Heavy exertion can result in collapse and unconsciousness at <79 mmHg PO₂ (ASTM, 2019). Below 16 % O₂, there is cognitive impairment that can lead to reduced risk recognition and poor decision making that has been implicated in many deaths (Spelce et al., 2016).

Data from volcanic fumarole studies have focused on the composition of fumarole gas from direct sampling to forecast magmatically driven eruptions—as a volcanic system reactivates, the gas emissions evolve from CO₂-rich to SO₂-rich (Stix and de Moor, 2018). In open atmospheres, volcanic gas concentrations expectedly decrease with distance from fumaroles. The confined space of glaciovolcanic caves reduce the dispersion of gas emitted from subglacial fumaroles.

Accumulations of concentrated volcanic gas in the Mount Rainier fumarolic ice caves have not been reported previously. First reports of volcanic gas by Stevens (1876) noted sulfurous fumes and steam vents along the north rim of the West Crater. More expansive observations of these fumes were reported by Ingraham (1895), Coombs (1936), and Kiver and Mumma (1971). Fumarole sampling in the East Crater during 1982 revealed elevated CO₂ (1.4 % to 4.2 %) and sulfur gasses below the detection level of 0.5 ppm (Frank, 1995). Zimbelman et al. (2000) reported ambient air in most cave locations on the summit as typical; however, fumarole emissions had CO₂ enrichments of 7 times to nearly 30 times that of air, trace H₂S odors were detected in the West Crater cave, and sulfate minerals encrusting a fumarole vent indicated locally high H₂S or SO₂ in the past. Separately, Le Guern et al. (2000) reported CO₂ concentrations near 300 ppm in the East Crater Cave atmosphere, and near 3000 ppm in the West Crater Cave atmosphere with H₂S concentrations of 2 ppm to 5 ppm in the West Crater Cave, below toxic levels.

Addressing their findings, Zimbelman et al. (2000) noted the need for further study of the risk of asphyxiation and CO₂ poisoning in the Mount Rainier caves. Curtis (2016) reported that gasses in fumarolic ice caves will be well mixed due to advection and CO₂ concentration is likely higher near the cave roof than the cave floor, therefore traps of CO₂ pooled near vents should not be a hazard to humans. With the previously unreported observation of large areas of IDLH CO₂ in West Crater Cave in contradiction with this, the existence of the phenomenon in the Mount Rainier cave system revealed environmental mechanisms that required better understanding. Badino (2009) concluded that gasses can accumulate in motionless atmospheres and create CO₂ traps in caves. As SO₂, H₂S, and CO₂ are less buoyant than air, the hazard is then expected to manifest in confined, poorly-ventilated spaces or the low-lying parts of the cave system.

The public, mountaineers, researchers, mountain rescue, and Mount Rainier National Park staff enter the fumarolic ice caves, therefore an assessment of hazardous atmospheres is necessary. We conducted repeat observations and gas measurements to determine the extent and persistence of volcanic gas present in the Mount Rainier cave systems and discuss in this paper the implications from a life-safety standpoint. The use of life support equipment enabled the full exploration of the cave system. We consider for the first time the reduction in O₂ concentrations due to displacement by volcanic gasses in fumarolic ice caves, and the combined effect with high altitude. Lastly, we measured airflow, air pressure, and fumarole output to understand the climatologic mechanisms and influences on CO₂-trap formation inside this volcanic subglacial environment. Understanding the connection between glaciovolcanic cave morphology and their atmospheres has further value as research into these unique environments continues from extra-terrestrial analog or volcanic hazard monitoring.

METHODS

Cave survey methods outlined in a comparison study of the long-term morphology of the Mount Rainier cave system in Stenner et al. (in review) produced detailed plan and profile maps. Survey data was reduced in COMPASS cave survey software. Cave room volumes used in calculations were computed in COMPASS by isolating survey data for two particular rooms and generating statistical reports. The room volume measurements are considered approximate.

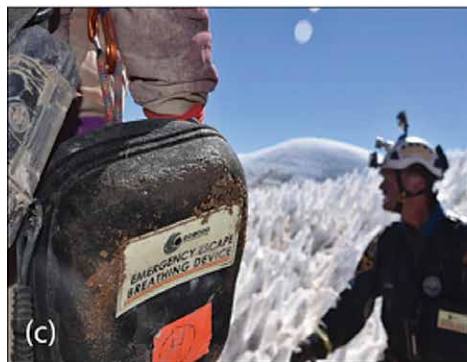
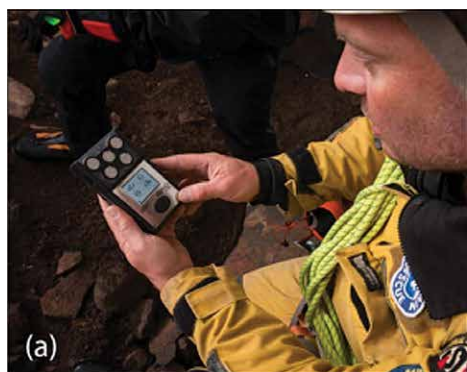


Figure 2. Methods. (a) Industrial Scientific MX6 iBrid portable gas monitor. (b) The West Crater Cave – preparing to take gas measurements using an aspirated MX6 iBrid gas monitor, hose attached to an avalanche probe above a zone of high CO₂. (c) Ocenco Self Contained Self Rescuer (SCSR) worn within the East and West Crater Caves as an emergency escape breathing device (EEBD). (d) Aspirated MX6 iBrid gas monitor mounted above a zone of high CO₂ Image: Wood, T. (e) Recording of cave floor surface temperatures using thermography. (f) Ultrasonic anemometer for detailed evaluation of air movements and flow.

software. Cave room volumes used in calculations were computed in COMPASS by isolating survey data for two particular rooms and generating statistical reports. The room volume measurements are considered approximate.

Environmental measurements were made in the caves which form the framework for gas dispersion. Long-term measurements included:

- Air temperature and relative humidity using data loggers (Geoprecision).
- Air temperature and pressure measurements between August 2016 and August 2017 near Lake Adélie in East Crater Cave (In-Situ BaroTroll).

Mobile measurements during expeditions included:

- Detection of H₂S, SO₂, CO₂ and O₂ throughout all cave passages during studies from 2015-2017 using calibrated Industrial Scientific MX6 iBrid gas monitors. O₂ and CO₂ measurements were displayed as percent concentrations and H₂S/SO₂ as parts per million. An aspirated version with a 10 m hose allowed measurement at low points, prior to descending into unknown atmospheres or in fumaroles, while staying above areas with hazardous concentrations representing IDLH (Fig. 2). Sensors were limited to an upper detection range of 5 % CO₂.
- CO₂ concentration in West Crater Cave was recorded from

August 1–5, 2017 using a CO₂-Probe GMP 251, (Vaisala) with an upper detection range of 20 %, combined with a DK390 rugged data logger (Driesen and Kern) for measuring air temperature, relative humidity, and atmospheric pressure.

- Quantitative and qualitative recording of cave floor surface temperatures using thermography (VarioCam High Resolution, Jenoptik) to record and evaluate single fumaroles, as well as whole fumarole fields (Fig. 2).
- Flow measurements using ultrasonic anemometers (USA-1, METEK) for detailed evaluation of air movements and the flow in the cave system (Fig. 2).
- Selected fumarole openings were equipped with a plastic tube and a hot wire probe (Testo). Gas velocity and temperature was measured, and volume flows were calculated based on gas velocity and the known diameter of the tube. Active fumaroles were fumaroles with a visible, audible, or palpable emission of gas.
- A mobile weather station (Vaisala WXT520) recorded the weather conditions outside the cave.

Where reported CO₂ values were over range (5 %) for detection equipment, gas concentrations were extrapolated from O₂ measurements using the formula in Spelce et al. (2016) adjusted to subtract from normal tropospheric O₂ % concentration, and two O₂ values were derived similarly from CO₂ measurements

$$(20.95 - z) = \frac{x}{5}, \quad (1)$$

where

- x = contaminant gas = $\frac{y}{10^4}$ (%)
- y = contaminant gas (ppm)
- z = measured O₂ (%).

This calculation provides the maximum possible contaminant gas concentrations and is subject to error, such as a potential mix of CO₂ and other possible contaminant gases such as N₂, Ar, or H₂S.

O₂ partial pressure (PO_2) values were derived from the atmospheric pressure using the formula

$$x = \frac{y(O_2)}{100}, \quad (2)$$

where

- x = PO_2 (% mmHg)
- y = atmospheric pressure (mmHg).

To complete the exploration of hazardous atmospheres, Self-Contained Breathing Apparatus (SCBA) was worn.



Figure 3. (a) Product image of Extreme Limited Access Breathing System (ELABS) Self Contained Breathing Apparatus (SCBA) showing thin confined space profile. (b) ELABS three carbon-fiber tank design, regulator, and air gauge/Rapid Intervention Team (RIT) quick fill connection. (c) Preparation to enter the “CO₂ Lake of Death” while wearing ELABS SCBA as life support equipment. (d) Descending into the “CO₂ Lake of Death” using ELABS SCBA as life support equipment.

This exploration of a confined space in a cold, volcanic environment, with a hazardous atmosphere comprising both dangerous levels of CO₂ and deficient in O₂ by concentration and by atmospheric pressure due to high altitude, presents a unique case. Life support equipment consisted of Extreme Limited Access Breathing System (ELABS) SCBA (Special Projects Operations, Inc.). The units are a modular, compact, pressure demand SCBA for confined spaces. A single manifold connects three carbon-fiber tanks which have a combined capacity of 1791 l gas at 4500 PSI. Total weight is 10.4 kg (Special Projects Operations, 2015) (Fig. 3). This project represented the first use of this equipment model in a cold high-altitude environment. ELABS were paired with an Avon FM53 full face mask. FM53 includes positive-pressure capability, an oro-nasal cup to reduce mask dead space, and has a rebreathed CO₂ value of 0.8 % (Avon, n.d.). Positive pressure in the mask is necessary to miti-

gate against leakage at the mask/facial seal. Additionally, each person wore an Ocenco Self Contained Self Rescuer (SCSR) as a backup emergency escape breathing device (EEBD) (Fig. 2). SCSR is a 1.6 kg self-contained belt-worn emergency breathing apparatus and can give a person a maximum of 15-32 minutes of breathable air to escape an area (Ocenco, n.d.). Two ELABS were worn for exploration with a third ELABS and backup air supply reservoir tank left in reserve at the base of the climb at Paradise trailhead.

Exploration of the most hazardous area was conducted using ELABS and included the following procedural methods. Exploration was on the second last day of the 2017 research deployment, which allowed four days and nights at the summit after two days of climbing to maximize acclimation and provide one additional day for contingencies. By this time research team members were partially acclimated, with blood oxygen saturation (SpO₂) levels, measured by pulse oximeter, having increased from 80–86 % to ~90 %. Acclimatization was further enhanced by prophylactic use of Acetazolamide prior to and during the ascent. Exploration was conducted with a rule of thirds protocol typical of cave diving

where one third of the available breathing gas is available for penetration, leaving one third for return and one third for contingencies. Testing prior to the expedition in a cave environment at 1400 m elevation revealed a 45 minute and one-hour ELABS tank capacity for Stenner and Graham, respectively, limiting penetration time to a maximum 15 minutes for the team. At the summit, a reduction in ELABS tank pressure of 300 PSI from maximum was noted. Additional safety mitigations included each team member wearing a climbing harness, use of a PMI reflective static rope and the pre-establishment of a fumarole rescue counterweight raise system (e.g., Cartaya, 2018). This system was secured above the hazardous atmosphere chamber with redundant ice screw anchors and manned by two team members and the expedition doctor. Medical O₂ and an Automated External Defibrillator were available.

RESULTS

Thermography revealed many areas on the East Crater floor with temperatures above the general surface temperature of about +2 °C to -2 °C as so-called hotspots. These ranged from small holes with temperatures of up to 59 °C to larger areas with temperatures ranging from 2 °C to 25 °C. Small but very hot spots were small fumaroles, while the larger areas were heated sediments or rock blocks. All active fumaroles were found to have vent temperatures above 40 °C and inactive fumaroles had temperatures up to 30 °C. The hottest fumarole had a degassing temperature of 59 °C. Figure 4 shows a typical fumarole

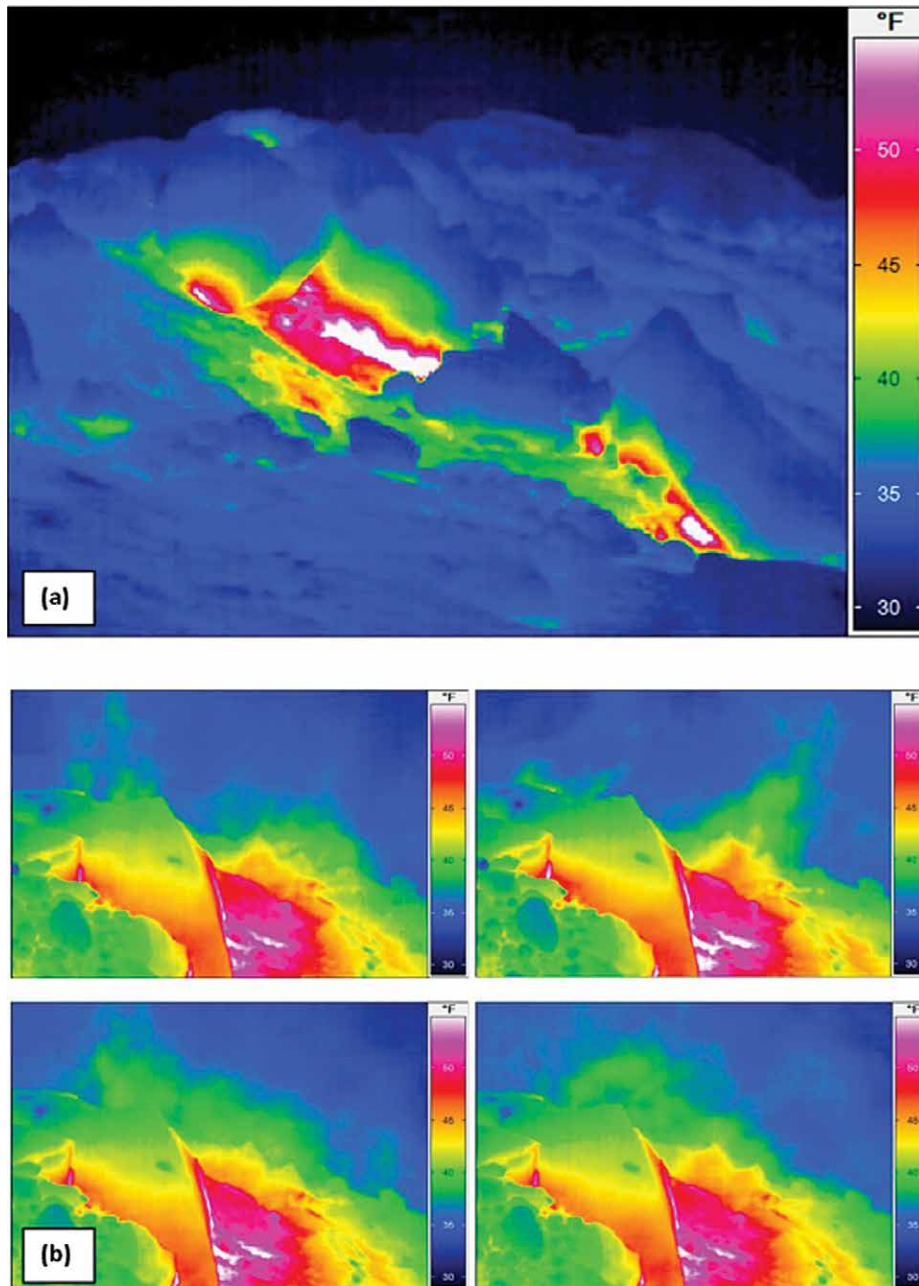


Figure 4. Thermographic images of fumarolic activity. (a) Thermographic image of a fumarole field in the main passages of the East Crater Cave system of Mt. Rainier without visible outgassing. (b) Thermographic image series showing the outgassing of water vapor above an active fumarole in the East Crater Cave system of Mt. Rainier.

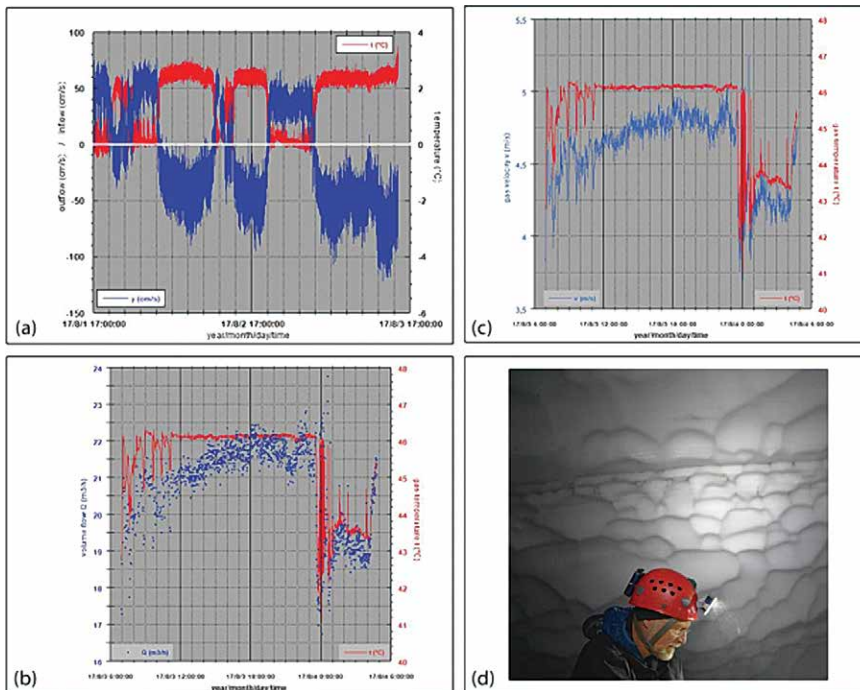


Figure 5. East Crater Cave climatologic and fumarole information. (a) Ultrasonic anemometer airflow (cm/s) and air temperature (°C) from passage junction below High Noon Entrance with alternating inflow (cold) and outflow (warm). Measurement interval: 1 sec. (b) Gas volume and temperature measurements of the fumarole near the Coliseum at survey station 1.42. (c) A possible warm air trap. The change of the scallop patterns at the transition from the side walls to the ceiling may show a change in airflow. (d) Gas velocity and temperature measurements of the fumarole near the Coliseum at Survey station 1.42.

field with small hotspots and the heated area around them. Degassing was visible at some hotspots due to water vapor condensing in the cold cave air. The zone of elevated CO_2 was approximately 40 cm in depth and confined to the trough. Two passages were noted with a maximum reading between 1.5 % to 1.6 % CO_2 , the Bird Grotto and the Low Loop. Both Bird Grotto and Low Loop begin as a low crawl way branching from the main passage and descending at a slope of 35–40 degrees. There was no distinct planar boundary, with CO_2 concentrations slowly increasing as the passages descended after branching off from the main passage

The Belly of the Beast differs, as it is a large, open room with a sloping floor of 35–40 degrees, terminating in a steeper slope near its lowest point. A measurement taken 7 m above the lowest point in the chamber found an 18.9 % O_2 concentration. The displacement of O_2 here is estimated to be by 10.3 % CO_2 , well above IDLH levels even at this point 7 m above the base of the chamber, which was not measured. East Crater Cave ambient air gas measurements are described in Table 1. IDLH areas are identified in Figure 6.

The Canary Room in the West Crater Cave was observed to have a persistent CO_2 trap whereby CO_2 concentrations were over detection range (over 5 %) and O_2 was under 18 %, stopping exploration in both 2015 and 2016 (Fig. 7). In the same years, measurable levels of SO_2 were observed at 0.3 %, and a trace scent of H_2S below monitor detection range. The hazard remained persistent in 2017 and exploration continued using ELABS. Using this equipment further penetration was focused on a downclimb into a dome shaped chamber with an apparent continuation, described during expeditions as the CO_2 Lake of Death (Fig. 3). Notable is the initial descent into the chamber, which was not strenuous, causing an increase in heart rate in the senior author to 178 beats per minute (BPM), in contrast to a resting heart rate of 90 BPM on the morning of the descent, both measured by wrist heart rate monitor. The chamber was explored, surveyed, and consisted of a single room with breakdown block and sediment floor. The apparent continuation became low, pinched out, and was not a viable passage. No obvious fumarole activity was noted. In 2017 the O_2 level in the CO_2 Lake of Death room was 16.0 %, and CO_2 measured over range for detection equipment. The displacement of O_2 is estimated to be by 24.8 % CO_2 , the highest ambient concentration in the Mount Rainier cave system. No H_2S or SO_2 was detected in this area. The West Crater cave ambient air gas measurements are described in Table 1 and IDLH areas are identified in Figure 8.

Discussion of hazards can be furthered by accounting for displacement of O_2 by CO_2 . Atmospheric air pressure recorded in the East Crater cave system during the study period reported by Florea et al. (2021) ranged from 426.7 mmHg

Strong degassing with visible and audible steaming was uncommon, while wide fumarole fields of hotspots were more prevalent. An example of clear water vapor degassing can be seen in the thermographic Figure 4. Here, the sequential images show the movement of the water vapor, which could only be detected as hot vapors up to a maximum of 1.5 m above ground. In the East Crater cave system there are only a few fumarole sites (<10) with strong degassing. A selected fumarole displayed volume flows between August 3, 2017 and August 4, 2017, of 16.7 m^3/h to 23.8 m^3/h . The volume flow as well as the degassing temperature is shown in Figure 5.

Measurements of gases in ambient air and our calculations to derive CO_2 concentrations revealed the following. In the East Crater Cave, ambient air in the main passages typically comprised 20.95 % O_2 and <0.3 % CO_2 . One reading in the main perimeter passage reached a maximum of 1.6 % CO_2 at a low point in the passage. This reading was specific to the

Table 1. Ambient air gas concentrations of areas inside the Mount Rainier Fumarolic Ice Caves, 2015–2017.

Cave	Passage Name	Date	Gas Concentrations, %				PO ₂ ^a (mmHg)	Notes
			CO ₂	O ₂	SO ₂	S		
East Crater	Main passages	08/2017	<0.3	>20.9 ^c	>89.1	Obs. maximum
East Crater	Main passage	08/2015	1.6	20.6 ^c	88.0	
East Crater	Bird Grotto	08/2017	1.6	20.6 ^c	88.0	
East Crater	Belly of the Beast	08/2015	10.3 ^b	18.9	80.6	7 m above floor
East Crater	Low Loop	08/2017	1.5	20.7 ^c	88.1	
West Crater	Canary Room	08/2017	15.3 ^b	17.9	76.4	
West Crater	CO ₂ Lake of	08/2017	24.8 ^b	16.0	68.3	
West Crater	Entrance	08/2016	0.3	
West Crater	Entrance	08/2017	0.3	
West Crater	Main passage	08/2015	Trace ^d	...	
West Crater	Main passage	08/2017	Trace ^d	...	
West Crater	High passages	08/2015	0.25	20.9 ^c	89.1	

^a Partial pressure values given for O₂ concentrations only. Values are assuming lowest recorded in cave air pressure measurement of 426.7 mmHg at O₂ 20.95 %.

^b Concentrations are extrapolated from O₂ measurements.

^c Concentrations are extrapolated from CO₂ measurements.

^d Scent detected but was below detection range for monitoring equipment.

to 462 mmHg. PO₂ is therefore between 89.3 mmHg and 97 mmHg assuming 20.95 % atmospheric O₂ concentration in the main passages. Accounting for the lowest observed atmospheric air pressures and the displacement of O₂ by CO₂, the lowest PO₂ in East Crater Cave was 80.6 mmHg and 68.3 mmHg in West Crater cave. These values assume that no other contaminant gasses than CO₂ are present to cause O₂ displacement and do not account for displacement by water vapor in the cave atmosphere, considered a small effect at 2 °C.

The Canary Room and CO₂ Lake of Death room in West Crater cave exhibited a distinct invisible planar boundary between safe and IDLH atmospheres. Normal ambient air gas concentrations of 20.95 % O₂ sharply degraded in the span

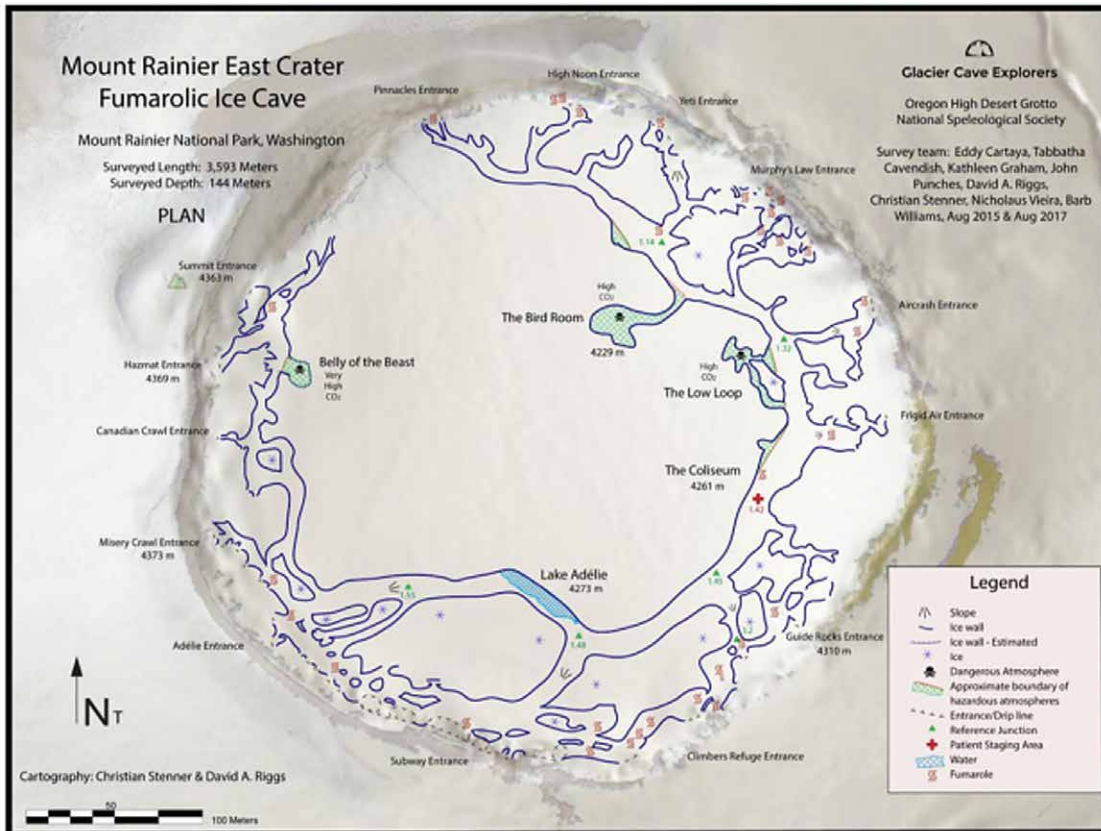


Figure 6. Survey in plan view of the East Crater Cave with zones of IDLH atmospheres identified. Map legend lists key features. Base map is a combination of digital elevation hillshade and satellite imagery.

of 0.3 m of elevation loss to 16 %, the lowest concentrations recorded. Symptoms of one support team member who briefly moved his head below the threshold unprotected described normal breathing suddenly interrupted by tunnel vision and a rapidly declining level of consciousness. The Canary Room exhibited an IDLH CO₂ trap over 3 m in depth (Fig. 7). Repeated measurements during our early expeditions showed the exact elevation of boundaries between IDLH atmospheres and breathable ambient air was variable.

To understand the CO₂ lakes in this

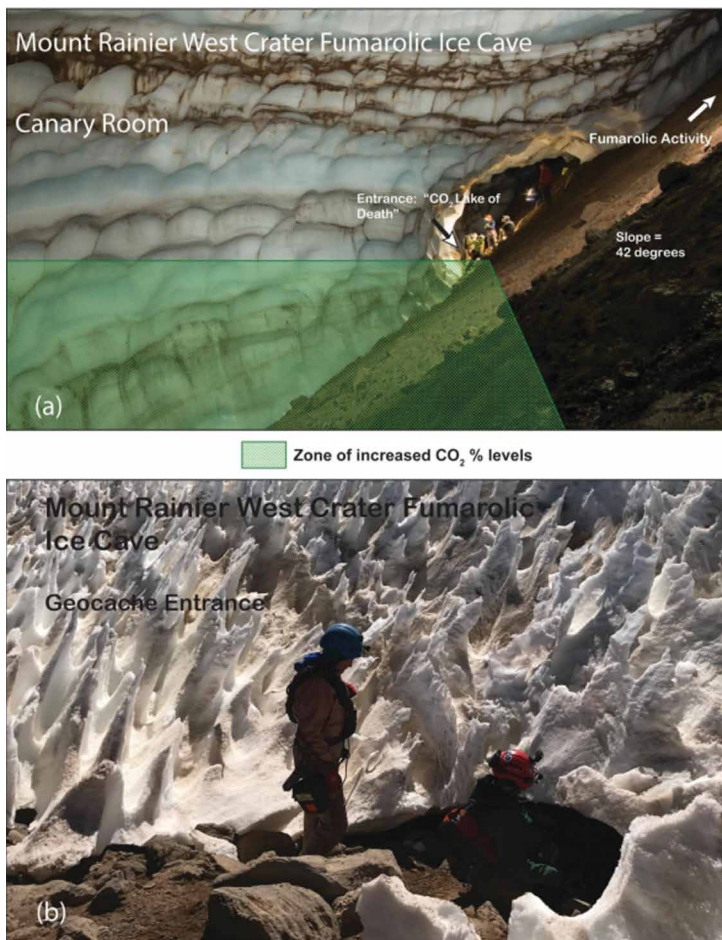


Figure 7. (a) A view across the Canary Room of the West Crater Cave, with the approximate planar boundary of IDLH CO_2 atmosphere identified. The room dimensions are 23 m \times 26 m \times 17 m (L \times W \times H) and not easily recognized as a confined space trapping CO_2 . (b) The "Geocache" entrance to West Crater Cave. This entrance is typical of the West Crater Cave entrances alongside the crater rim.

temperature. Thus, air pressure can be identified as the main influencing factor on the CO_2 level. The correlations of the individual measured variables to the CO_2 concentration can be seen in Figure 9b, c and e. By calculating the cross-correlation between CO_2 concentration and air pressure, an increase of the correlation to Pearson R of nearly -0.80 can be achieved with a shift of 7.6 hours (Fig. 9f); there is no improvement for humidity and only an insignificant improvement for air temperature.

However, a change in the CO_2 concentration several hours before a change in air pressure makes no sense from a scientific point of view. Instead of a pressure change the change in CO_2 concentration can be explained by a drop in the air temperature as observed in the temperature collapse on August 3, 2017 at 22:15 to August 4, 2017 at 05:45, which disturbs the concentration-pressure correlation and creates the 7.6-hour shift.

In a second step, the time series was divided and only the first part, prior to the temperature drop, was examined more closely until the temperature drops (Fig. 9g). Here, Pearson R : values of -0.77 and $R1$ of 0.60 are obtained (Fig. 9h). The cross correlation did not yield better values when the time series were shifted (Fig. 9i).

DISCUSSION

The proximity of mountaineers to the cave system puts them in the vicinity of hazards in addition to those of regular mountaineering. As the caves have been entered by climbers for shelter in bad weather, or out of curiosity, safety information is necessary given our findings. Currently there is no public facing information by the National Park Service directed towards climbers regarding the cave system warning about hazards. Notwithstanding the fact that gas concentrations near source fumaroles are considerably higher and a known hazard, our findings indicate ambient air in the caves is a serious concern.

region of West Crater Cave, a CO_2 sensor was installed at the approximate boundary of safe and IDLH atmosphere during the 2017 expedition, which records the CO_2 concentration (%) every second. Additionally, the air temperature, relative humidity, and the atmospheric pressure inside the cave were recorded. The measured data are summarized in Figure 9. It is noticeable that the CO_2 concentration seems to oscillate during the first half of the measurement period. Relatively long phases of higher CO_2 concentrations are repeatedly interrupted by significant drops of 2 % to 5 %. Both the relative humidity and the air pressure show a similar pattern, but with opposite tendencies, while the air temperature seems to have no influence. The CO_2 dips are accompanied by increasing air pressure and increasing humidity values.

In the second part of the measurement, there is a significant change. The air pressure drops rapidly at first, then somewhat more slowly without the previously oscillating fluctuations. The course of the CO_2 concentration responds with a noticeable increase at first, followed by sudden collapse before it stabilizes again at a high level. The decreasing concentration towards the end of the measurements is not considered further. The reason for the strong decrease of about 3.5 % is not explained by air pressure fluctuations. Rather, it coincides with a significant temperature drop of >1.5 $^{\circ}\text{C}$, which is unique for this short measurement series.

Examining correlation calculations for the entire measurement series in Figure 9d, the best correlation by far is between CO_2 concentration and air pressure of approximately Pearson R : -0.70 , while only Pearson R : -0.35 is achieved between CO_2 and relative humidity and just Pearson R : 0.18 in relation to temperature.

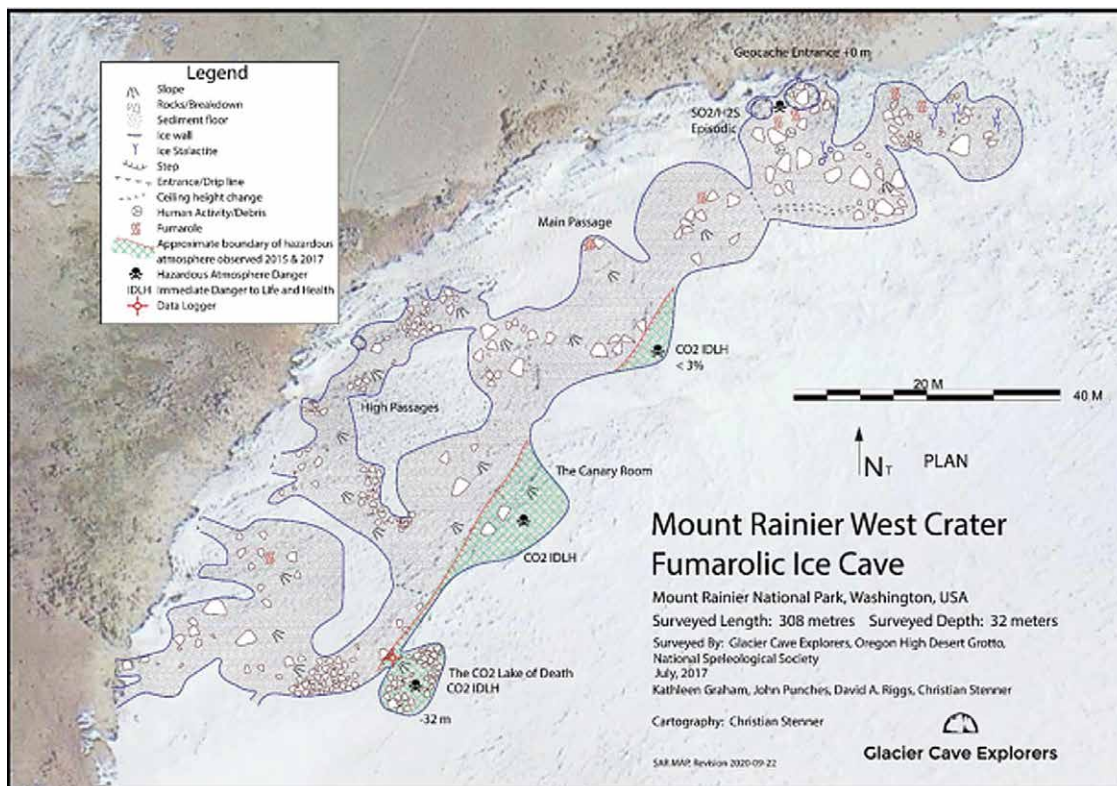


Figure 8. Survey in plan view of the West Crater Cave with zones of IDLH atmospheres identified and indicating the CO₂ data logger location. Map legend lists key features. Basemap is from satellite imagery.

gasses. Measurements throughout the new Mount St. Helens fumarolic ice caves revealed a maximum of 0.3 % CO₂ (Sobolewski et al., 2020). On Mount Hood volcano a hydrothermally-influenced ice cave contained no volcanic gas (Pflitsch et al., 2017).

Contrasting these results is the well-known fumarolic pit on Mount Hood (Tomlinson, 2019). Known as Devil's Kitchen, analysis reported by Nehring et al., (1981) reported CO₂, H₂S, and O₂ measurements from fumarole sampling in the pit of up to 94.4 %, 3.9 %, and 0 %, respectively. High CO₂ concentrations also exist at Mammoth Mountain Fumarole. Direct sampling revealed CO₂ 98.7 %, O₂ 0.09 %, H₂S, 0.02 %. After the fatalities there, ambient air measurements taken one to two hours following the incident revealed O₂, 18 %, CO₂, 10 %, CO, 4 %, and H₂S, 0.003 % (Cantrell and Young, 2009). Limited information on Mount Baker summit crater reported the presence of fumarolic ice caves and measurements from 1974–1977 of CO₂ from 14.4 % to 36 % maximum and H₂S 0.0074 % to 7.4 % maximum, levelling off at 3.8 % (Kiver, 1978). Adding to this, our data shows that CO₂ emitting fumaroles have caused CO₂ accumulations to form where they had not previously been noted in the Mount Rainier caves, suggesting the possibility of such accumulations to be dynamic due to variable ventilation and fumarole output. Also, that this phenomenon can persist in fumarolic ice caves, even those with ventilation effects such as the Mount Rainier system.

Mount Rainier cave hazardous atmospheres

The Hazmat entrance to East Crater Cave is near Columbia Crest and is an attractive curiosity easily visible to mountaineers. Within, the steep slope descends to the base of the passage at Belly of the Beast where the highest CO₂ concentrations are recorded in East Crater Cave (Fig. 10). Even the main passages, which held a trough of CO₂ adjacent to debris ridges, could be a hazard in the case of a person who slips on the steep slopes and lands with their head and airway in a hazardous atmosphere. The entrance to the Bird Grotto and Low Loop are tight and unlikely to be visited, except for persons who may want to explore the lowest point in the cave. The West Crater Cave is a significant concern due to the highest levels of CO₂ observed, an attractive curiosity (geocache) at a fumarole known to vent SO₂, and little ventilation observed during the expeditions that would assist in dispersal of fumarole gasses. Our measurements across expeditions reveal another danger in that the location of the IDLH atmosphere boundary is inconsistent and cannot be reliably defined, making communication of exact zones of IDLH atmospheres difficult. The Canary Room is a considerable hazard. Within, a person can walk across a large, open chamber on the sloping cave floor with their head, gas monitor, and airway in safe air, and their knees in IDLH atmosphere. A layperson would not recognize the vast room as a confined space and the potentially lethal consequence of walking along the bottom (Fig. 7).

Other glaciovolcanic cave systems have typically revealed low concentrations of volcanic gas in ambient air. Studies by Ilanko et al. (2019) at Mount Erebus, Antarctica, caves using various methods found vent samples over 2 % CO₂ and ranging up to 2.9 %, but ambient air concentrations of up to 0.94 % CO₂. Curtis (2016) found up to 2 % CO₂ inside Warren Cave at Mount Erebus. Studies at Sandy Glacier on Mount Hood and on Mount St. Helens reveal none or only traces of CO₂ in safe amounts and no other volcanic

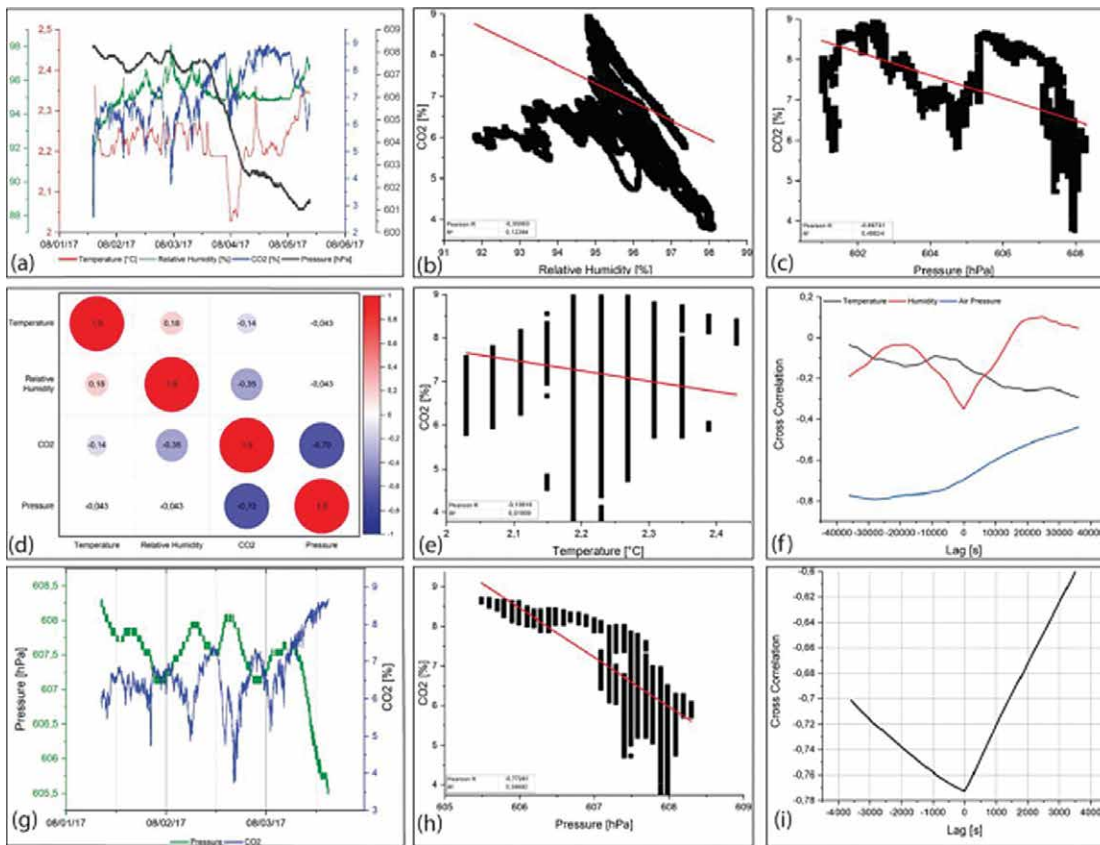


Figure 9. Graphs of measurements inside the West Crater Cave of Mt. Rainier, WA, USA. Measurement interval: 1 sec. The air temperature data were smoothed hourly for better visualization by the method of Savitzky & Golay (1964). (a) Course of the measurement parameters temperature (°C), relative humidity (%), CO₂ content (%) and atm. air pressure (hPa) during the measurement period of August 1 to August 5, 2017. (b) Results of the linear correlation between CO₂ (%) and rel. Humidity (%) during the measurement period of August 1 to August 5, 2017. (c) Results of the linear correlation between CO₂ (%) and atm. air pressure (hPa) during the measurement period of August 1 to August 5, 2017. (d) Summarized results of correlation analyses of all measured variables based on Pearson's correlation coefficient. (e) Results of the linear correlation between CO₂ (%) and air temperature (°C) during the measurement period of August 1 to August 5, 2017. (f) Results of the cross correlation between CO₂ (%) and atm. air pressure (hPa), rel. humidity (%) and air temperature (°C) during the measurement period of August 1 to August 5, 2017. (g) Course of the measurement parameters CO₂ content (%) and atm. air pressure (hPa) during the measurement period of August 1 to August 3, 2017. (h) Results of the linear correlation between CO₂ (%) and atm. air pressure (hPa) during the measurement period of August 1 to August 3, 2017 (i) Results of the cross correlation between CO₂ (%) and atm. air pressure (hPa), rel. humidity (%) and air temperature (°C) during the measurement period of August 1 to August 3, 2017.

concentration below 19.5 % by volume, which it considers IDLH. However, human performance and survival at high altitudes and O₂-deficient atmospheres is more substantially affected by the amount of biologically available oxygen based on PO₂. (Spelce et al., 2016). ASTM (2019) considers this, and in this standard, IDLH atmospheres include where total atmospheric pressure is less than 584 mmHg (77.86 kPa) equivalent to 2134 m altitude or any combination of reduced percentage of oxygen and reduced pressure that leads to an oxygen partial pressure less than 122 mmHg (16.27 kPa). Atmospheres with PO₂ ≥ 122 mmHg and less than 148 mmHg are oxygen deficient but not IDLH. (ASTM, 2019).

Air at the summit is O₂ deficient for unacclimated individuals and can be further exacerbated by reductions in O₂ concentration due to displacement by volcanic gasses in the caves. CO₂ concentrations in some areas are not considered toxic as they are below the OSHA IDLH level of 4 %, such as the Low Loop and Bird Grotto in East Crater Cave. However, considering the displacement of O₂ and reduced PO₂ at altitude these areas are considered IDLH for unacclimated persons as per the 122 mmHg level in ASTM (Table 1), which has implications for researchers or rescuers who may respond to trauma or asphyxiation underground and would require wearing SCBA for life safety.

Implications of the reduced PO₂ include the effect on SCBA users, as SCBA do not overcome O₂ deficient atmospheres very well at high altitude, and maximum in mask pressures during expiration are only 6.5 mmHg above ambient (McKay, 2020). Additionally, inside the facepiece, CO₂ can range in concentration from 2 % to 5 % (Spelce et al., 2016). As full-face mask SCBA with fills of regular O₂ concentration are not likely to elevate PO₂ higher than the IDLH level of 122mmHg in unacclimated individuals, entry into the Mount Rainier caves or others with contaminant gases at high altitudes is a fac-

The obvious IDLH atmospheres due to high concentrations of volcanic gasses, as per CDC or OSHA requirements, must not be considered alone. Areas of seemingly low concentrations of CO₂ such as the Bird Room and Low Loop in the caves can be IDLH when considering O₂ displacement and PO₂ due to the high altitude. Literature does not reveal information on O₂ displacement in fumarolic ice caves, probably because where volcanic gasses displace O₂ in significant amounts the hazard would likely manifest first in the displacing gasses. With increasing altitude, the atmospheric pressure decreases, and the amount of O₂ molecules available for respiration decreases as well (Spelce et al., 2017). The OSHA respirator standard defines O₂-deficient atmospheres as having an oxygen concentration below 19.5 % by volume, which it considers IDLH. However, human performance and survival at high altitudes and O₂-deficient atmospheres is more substantially affected by the amount of biologically available oxygen based on PO₂. (Spelce et al., 2016). ASTM (2019) considers this, and in this standard, IDLH atmospheres include where total atmospheric pressure is less than 584 mmHg (77.86 kPa) equivalent to 2134 m altitude or any combination of reduced percentage of oxygen and reduced pressure that leads to an oxygen partial pressure less than 122 mmHg (16.27 kPa). Atmospheres with PO₂ ≥ 122 mmHg and less than 148 mmHg are oxygen deficient but not IDLH. (ASTM, 2019).



Figure 10. East Crater Cave. (a) View from just below the Mt. Rainier summit (Columbia Crest) towards glacio-volcanic cave entrances. “Hazmat Entrance” of the East Crater Cave. Descending from the Hazmat entrance is steep passage terminating at the “Belly of the Beast” area of highest CO₂ concentrations recorded in the East Crater Cave system. (b) “Summit Entrance” passage connects to the “Hazmat Entrance” passages and terminate at a low point “Belly of the Beast”. Both entrances are visible to the public from the East Crater side of the crater rim just below Columbia Crest. (c) Coliseum room and master passage circumnavigating the East Crater Cave. (d) Fumarolic area in cave entrances near the East Crater rim.

tor to consider. The solution is to use acclimated personnel or use O₂ enriched air fills. Complete acclimatization requires about four weeks’ residence at the ambient PO₂ (Spelce et al., 2016; McKay, 2020). ASTM (2019) requires at least 23 % O₂ at 3048 m (air pressure <523 mmHg) and 27 % O₂ at 4267 m (air pressure <450 mmHg) to provide the same amount of O₂ in the tracheal region of the lungs that is available for biological processes as one would receive by breathing ambient air at sea level (Spelce et al., 2016).

Although these cave atmospheres are primarily IDLH

due to CO₂, we seek to quantify the impact of reduced O₂ to those who are acclimated or only partially acclimated such as in our case. One way would be to extrapolate the low PO₂ of the O₂ deficient areas to an equivalent altitude above sea level. As SCBA will only add 6.5 mmHg above ambient pressure this assists in understanding the potential physiological effects of reduced PO₂ even when fully protected against contaminant gases. To model and compare O₂ deficient areas with atmospheres at regular tropospheric O₂ concentrations and various altitude dependent pressures we adapt the barometric formula (Berberan-Santos et al., 1997). However, using the previous ratio to calculate the equivalent atmospheric pressure of reduced cave PO₂ as if in a normal atmosphere of 20.95 % O₂ at 426.7 mmHg, substituting those values for *P* and solving for altitude (*h*)

$$P = P_b \left[\frac{T_b}{T_b + L_b(h - h_b)} \right]^{\frac{g_0 - M}{R \cdot L_b}}, \tag{3}$$

where

P = Equivalent air pressure (Pa)

P_b = reference pressure (Pa): 101300

T_b = reference temperature (K): 275.15

L_b = temperature lapse rate (K/m) in International Standard Atmosphere: -0.0065

h = altitude of *P* (m)

h_b = altitude of reference, sea level (m)

R^* = universal gas constant: 8.3144598 J/(mol·K)

g_0 = gravitational acceleration: 9.80665 m/s²

M = molar mass of Earth's air: 0.0289644 kg/mol.

The equivalent altitude of O₂ deficient cave atmospheres is calculated using the PO_2 as determined for each passage, using the low of 426.7 mmHg in cave air pressure and an average in cave temperature of 2 °C (Florea et al., 2021). Table 2 compares actual altitudes of O₂ deficient passages and their PO_2 with others and allows comparisons to be made.

Table 2. Comparison of O₂ deficient Mount Rainier Cave passages and their equivalent altitudes.

Location	Altitude (m)	Temp. (°C)	O ₂ (%)	Atmospheric Pressure (mmHg)	PO ₂ (mmHg)	Equivalent Atm. Pressure ^a (mmHg)	Equivalent Altitude (m)
Comparison Locations							
Sea Level	0	15 ^b	20.95	760.0	160.0	760	0
Rainier Paradise Center	1646	15 ^b	20.95	625.3	131.0	625.3	1646
Mount Rainier Summit	4392	0 ^b	20.95	438.9	91.9	438.9	4392
Mount Everest Summit	8848	-19 ^b	20.95	231.5	48.5	231.5	8848
Mount Rainier Cave Passages							
Main passage trough	4269	2	20.4	426.7	87.0	415.0	4779
Bird Grotto	4230	2	20.4	426.7	87.0	415.0	4779
Belly of the Beast	4344	2	18.9	426.7	80.6	384.7	5487
Low Loop	4260	2	20.4	426.7	87.1	415.8	4770
Canary Room	4355	2	17.9	426.7	76.4	364.7	5950
CO ₂ Lake of Death	4350	2	16.0	426.7	68.3	326.0	6821

^a Atmospheric pressure of reduced PO_2 extrapolated to a normal atmosphere of 20.95 % O₂ at 426.7 mmHg.

^b Temperatures used as estimates to calculate air pressure and PO_2 values for comparison.

In addition to the primary hazard of contaminant gases, exposure to reduced PO_2 results in experiencing an equivalent felt altitude increase of 510 m in Low Loop, 1143 m in Belly of the Beast of East Crater Cave, and a worst-case increase of 2471 m from actual in West Crater Cave CO₂ Lake of Death. The O₂ deficiency could be a potential factor for the heart rate increase of 88 beats per minute in the senior author as only partially acclimated during the study. Were it not for the fact that O₂ deficiency in some cases is caused by IDLH levels of CO₂, regular mountaineering O₂ and masks would be sufficient protection. SCBA with positive pressure full face masks to mitigate contaminant gas leakage is necessary. Partial acclimation due to conducting the summit climb over two days, three further sleeps at the summit and use of Acetazolamide likely assisted in negating negative symptoms of O₂ deprivation. Most mountaineers are more acutely exposed to the altitude and do not benefit from the same partial acclimation, or in case of helicopter transport may receive no acclimation.

Development of hazardous atmospheres in the caves

CO₂ traps would not exist if the positive buoyancy effect of vent gas heat content overcomes the negative buoyancy effect of vent gas composition, as discussed by Curtis (2016). We explore why CO₂ traps of IDLH form and persist in the Mount Rainier system. The CO₂ accumulations of 3 m and over 7 m deep appear to be an outlier in comparison to other glaciovolcanic systems, notwithstanding high CO₂ output fumaroles in blind unventilated pits such as Mammoth Mountain Fumarole and Devil's Kitchen which may conform to the situation described by Badino (2009). Strong ventilation effects inside the Mount St. Helens caves in combination with their morphology are a possible explanation why concentrations there are relatively low (Sobolewski et al., 2020). As well, at Mount Rainier the mostly impermeable crater floor of breakdown and sediment contrasts with the Mount St. Helens cave floors which consist mostly of stacked volcanic rocks with gaps between, thus providing more possibilities for CO₂ to accumulate and become trapped at Mount Rainier.

In this context of gas buoyancy, two effects must be considered: the degassing of the fumaroles, and the airflow conditions in the cave system and at passage junctions. It should be noted that degassing fumarole openings at Mount Rainier are usually not exposed, and degassing does not occur directly into the cave atmosphere but is hindered by

boulders or smaller debris. This causes the gas flow to diffuse rapidly and mix with the ambient air, which leads to cooling and condensation of the water vapor (Fig. 4). Furthermore, the rock/debris is heated and, in return, the escaping gas is cooled quickly. Another case that should not be underestimated occurs where fumaroles are in marginal areas to the glacier ice or in narrow pockets under the ice. There, escaping gas directly encounters the glacier ice and cools down rapidly. All this leads to a significant reduction in the buoyancy of the escaping gases. In addition, most fumaroles are located in the upper sloping passages close to the crater rim (Fig. 10) so a large part of the warm air is led directly outside.

A second important point is the general air flow in the cave system, which determines the air exchange with the outside atmosphere and the mixing of the fumarole gasses with the cave air. During the expeditions in 2015 and 2016 we observed periods of little air movement in the main annular tunnel of the cave system alternating with periods of strong air movement. A good indicator for this was the formation of fog. When the air was predominantly calm, very strong fog sometimes formed over the whole system, whereas when the air was well ventilated, the area was mostly clear. It was also observed that higher flow velocities and clear visibility were always accompanied by cold air intrusion from one or more of the numerous openings. In 2017, air flows were recorded for the first time using ultrasonic anemometers. In Figure 5a we see a recording of the flow situation, as well as the air temperature, measured at the junction below High Noon Entrance over a period of almost 3 days. The location is in the influence of the openings to the High Noon and Pinnacles Entrance (Fig. 6).

The most obvious feature is the continuous change of the flow direction with respect to the main tunnel's corridor axis. The changes in direction are also visible by the significant temperature changes. The data shows the inflow of cold air from Pinnacles Entrance into the cave system and the outflow of warmer air from the cave system towards Pinnacles Entrance. The air currents are clearly pronounced at 0.5 m/s to 1 m/s. These constant changes of direction confirm our direct observations from 2015 and 2016, where we observed that the respective flow situation appears to exist over the entire vertical extent. A vertically stratified flow with outflowing warm air in the ceiling area and inflowing cold air at the bottom would be considerably more stable. Furthermore, we never observed stratified layers of fog below the ceiling and clear air. The observed flow is caused by the complex interaction of the numerous openings of the system to the outside atmosphere, which have different tunnel morphologies. Many openings have significant narrowing in the upper area, which also speak against vertical stratification.

A good example of this is the fumarole at the Coliseum room, which yields the data in Fig. 5b and 5c. This fumarole is quite active, with audible, blowing steam and located in a widened tunnel section in the lower part of the conduit, 10 m below the ceiling. We measured a volume flow of around 22.1 m³/h over a twelve-hour period before the volume flow dropped to a lower level. Compared to the volume of the Coliseum room, which is approximately 10,500 m³, the fumarole exhaled 0.2 % of the room volume, or 2.5 % over the twelve hours.

Summarizing the results and observations of airflow and volume flow, it can be assumed that degassing CO₂ in the main passage of the cave is diluted and removed quite quickly due to low to moderate buoyancy. This process is supported by the morphology of the cave ceilings, which are partly inclined and form guiding paths to the entrances. CO₂ can only accumulate under the ceiling where bow-like morphological structures form traps for warm air.

An identifiable instance is the hall above survey station 1.14 below the Yeti and Murphy's Law entrances, with a volume of approximately 3,100 m³. Here the passage structure is interrupted by a dome-like deck and based on the ice structure a clear inversion limit can be determined (Fig. 5d). Especially the fumarole in the upper slope area, close to the ceiling, with a volume flow measured of about 26.5 m³/s up to 55.3 m³/s leading to a noticeable warm air convection.

In the lower area of the master passage; however, a small CO₂ lake was identified, which is fed by fumaroles lying deep below the boulders in the lower slope area. These CO₂ lakes are formed at the transition area to the glacier where the weak degassing cools down quickly and cold air with heavier CO₂ accumulates preferentially. The air currents passing through the ring system and the upward cave passages have no influence on these areas, so CO₂ can easily accumulate.

Figure 11a shows a situation in the main passage of the East Crater without strong compensation winds between cave and outside atmospheres. Fumarole degassing rises into the passage. Part of the gas rises to the outside in the next connecting tunnel while cooling down slowly while another part remains inside the tunnel under the ceiling and cools down as well. The cooling effects are achieved by mixing with the ambient air but also by contact with the ice surface on the walls and ceiling. The cooled air then sinks back down the walls and collects at the lowest point. Depending on the morphology of the tunnel, it can also lead to a rotational movement in the upper part. Since the buoyancy of the escaping gases is not strong enough, only part of the heavier CO₂ is carried up, while the remainder sinks down. Further CO₂ is transported by the cooled sinking air into the deeper passages and accumulates. The heavy cold air and the heavier CO₂ reinforce each other in the stabilization of the cold CO₂ lake.

Figure 11b shows the situation in the context of a massive inflow of cold air through the connecting passage to the outside. The heavy cold air flows through the entire cross-section of the corridor into the lower ring passage and mixes

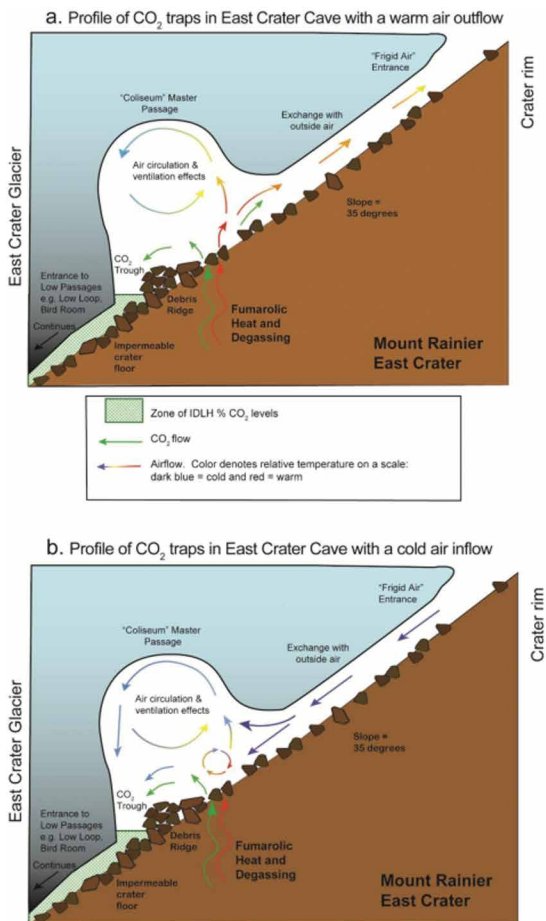


Figure 11. Cross section diagram of master passage as in the East Crater Cave coliseum passage area. The image shows the debris ridges as described by Kiver and Steele (1975) and trough of CO₂ as measured during 2015 and 2017 expeditions. (a) Shows the situation with a warm air outflow. (b) Shows the situation with a cold air inflow.

with the warm fumarole air, resulting in a temperature equalization between both flows. Since cold air also flows down to the fumarole, the cold air effect dominates, and cold air can further stabilize the CO₂ lake. The gases escaping from the fumarole cannot escape from the connecting corridor due to the massive cold air flow but are distributed in the ring passage, cooling down on walls and ceiling. The CO₂ will accumulate at low points and CO₂ lakes are likely to grow. The CO₂ lakes will dissipate only when advective currents (horizontal air flow through the tunnel) dominate and the air currents moving through the ring passage become dominant that can occur until the horizontal current can no longer reach the CO₂ lake significantly because flows are above it.

The same applies to passages below the main corridor like the Bird Room and the Low Loop. There the air exchange is considerably restricted, with the cold air remaining stable and the heavy CO₂ trapped in the whole room. Even if the cold air inflows are less frequent, the CO₂ accumulations will stabilize due to the following circumstances. The currents from the ring system do not penetrate into these lower passages and are not able to remove CO₂. Warm fumarole gases cool down relatively quickly on the surrounding walls and sink to the bottom, and only a small part of the CO₂ can escape by means of warm air, which is supported by the fact that the entire Bird Room has increased CO₂ levels and no clear layer boundary exists.

In the West Crater Cave, even though the series of measurements is short and cannot be considered representative, they provide interesting information on the climatological framework conditions and their effect on the CO₂ lake (Fig. 9).

Since the measurements were taken at the edge of the CO₂ lake, the detected concentration fluctuations are likely based on the following mechanisms. The boundary layer of the CO₂ lake may shift slightly downwards with increasing atmospheric pressure, which would be shown by an immediate decrease in concentration. Or, fumarole activity is dependent on atmospheric pressure and the volume flow from the fumaroles decreases with increasing air pressure, so that expansion of the lake is reduced by a lower recharge. In this case, the concentration changes are likely to show a time lag, which has not been observed.

The decrease in humidity will probably be caused by different moisture content of the cave atmosphere and the CO₂ lake. In the upper cave passages, the water vapor-rich fumarole gasses condense and simultaneously rise to the surface, and an accumulation of humid to even misty air masses will occur, while the CO₂ lakes will be influenced more so by the sinking, drier, and CO₂-rich air.

The marked drop in CO₂ concentration combined with a significant drop in temperature on 3 and 4 August is probably due to the intrusion of cold air masses through one of the entrances and thus a shortage of flow. Here, short-term, inflowing, colder outside air leads to dilution of the CO₂ concentration, but at the same time to a stabilization of the CO₂ lake, because the cold air strengthens the inversion.

Our hypothesis about the environmental conditions and processes in the West Crater are shown in Figures 12 and 13. Figure 12a shows the most common situation where part of the degassing escapes directly to the outside, while the other part cools down at the ceilings and walls and sinks to the bottom. While the cooler air moves directly to the lower areas, the slightly warmer air rises to the top, cools down under the ceiling and sinks to the bottom at the ice wall at the lower end. The heavy CO₂ supports this movement. There are no buoyancy forces to start circulation. Also, the strong compensation currents between the outside atmosphere and the cave, as seen in the East Crater, seem to be missing. This is probably due to the much smaller openings to the outer atmosphere but also to the morphology of the West Crater passages that have neither the structure nor the size of the ring system of the East Crater.

Figure 12b shows the situation in the context of a less frequent cold air intrusion. Here, a large part of the fumarole output is forced downwards. While the ground-level cold air flow with part of the CO₂ is led into the cold CO₂ lake, part of the warm gas rises into the ceiling areas and cools down slowly. However, the descending air is still lighter than the

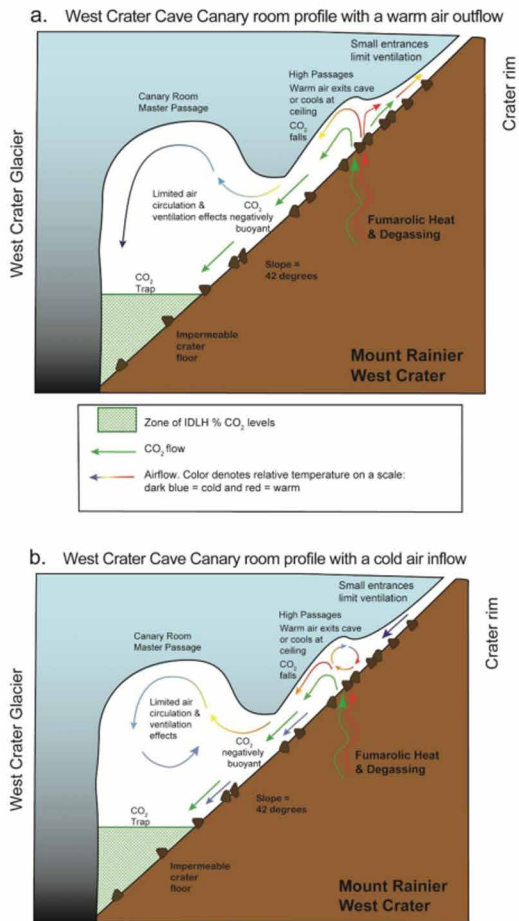


Figure 12. Cross section diagram of Canary Room as in the West Crater Cave showing conceptual CO₂ trap formation. Degassing fumaroles higher in the cave passages vent heat and CO₂ which pools due to low ventilation effects and buoyancy loss. (a) Shows the situation with a warm air outflow. (b) Shows the situation with a cold air inflow.

It is possible that changes in fumarole output or cave morphology have caused the CO₂ traps to form in the 20–49 years since the previous studies. Even though toxic levels of volcanic gasses were not always noted in previous studies, these new measurements do not necessarily reflect a change in volcanic degassing, as our results are the first systematic recording of ambient air gas levels throughout the entire cave system. Continued study of this unique environment could include habitability for microorganisms in CO₂ rich areas, given the possible Mars analogue this dark, low nutrient, low-pressure, high CO₂ environment presents. Additional climactic measurements or modelling would help understand and validate the mechanisms of CO₂ trap formation and persistence. Public education on gas hazards could also bring beneficial information such as climbers noting sulfurous odors from East Crater, denoting a change in the magmatic system.

CONCLUSIONS

Fumarolic ice caves are not heavily studied, thus detailed studies of these cave systems must include numerous case examples. In addition to the general hazards of mountaineering, cave exploration, and the remote environment, the toxic levels of CO₂ and variability of hazardous atmospheres, outline caution required of anyone entering the Mount Rainier fumarolic ice cave system, particularly in areas where the morphology and fumarole output increases the manifestation of hazardous atmospheres. The formation and persistence of CO₂ traps result from rapidly diffusing fumarole gas mixing with the ambient air, which leads to cooling and a significant reduction in gas buoyancy. Cave morphology and fumarole location also affect CO₂ accumulation in that narrow entrances and low ceilings limit airflow and cause cooling of vented gases. Low areas of East Crater Cave, including the Hazmat entrance below Columbia Crest, and

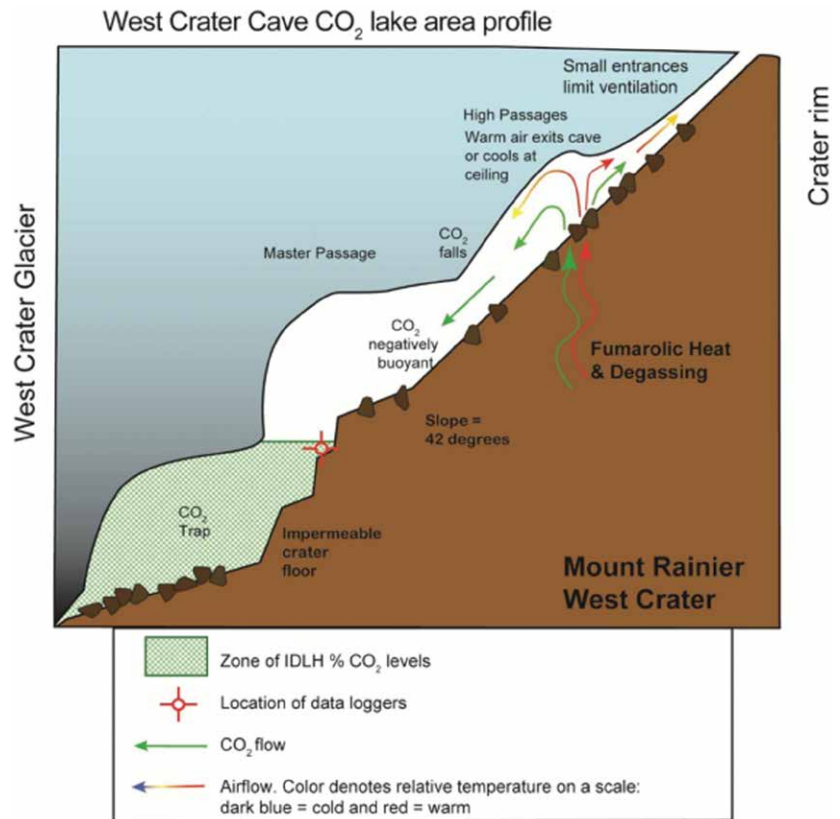


Figure 13. Cross section diagram of main passage CO₂ lake area as in the West Crater Cave showing CO₂ trap and data logger location. Degassing fumaroles higher in the West Crater Cave passages vent heat and CO₂ that pools due to low ventilation effects and buoyancy loss.

colder air of the CO₂ lake, which also has a higher CO₂ concentration, so that a rotational movement can occur when the descending air is again seized by the warmer air of the fumarole in the direction of the connecting tunnel to the outside.

The CO₂ concentration in the upper part of the CO₂ lake can be reduced. Fresh cold air flowing into the lake leads to a replenishment of the lake but also to a dilution of the CO₂ concentration. Even if the cold air carries further CO₂, its concentration is lower than in the CO₂ lake.

the West Crater Cave in general include significant, large areas of IDLH atmospheres. These areas do not present a consistent planar boundary, and have an appearance of voluminous, ventilated chambers that nevertheless trap hazardous gasses. In addition to areas of high CO₂ concentrations of up to 24.8 %, O₂ displacement and low atmospheric pressure add to the hazard. Acute exposure to the high-altitude environment by humans who may not have acclimated is exacerbated in the caves by the displacement of O₂ to create IDLH atmospheres even where CO₂ concentrations are not themselves toxic. The use of SCBA is necessary to protect against volcanic gasses, however the effect of the high altitude on PO₂ and limitations of SCBA systems impact the ability to maintain PO₂ above 122 mmHg in a full-face mask SCBA system at Mount Rainier. Low PO₂ in cave passages due to O₂ displacement combined with high altitude can equate to the equivalent PO₂ of much higher altitudes, which has implications for those working in high altitude glaciovolcanic environments. Education of climbers, researchers, and the public is important to prevent accidents and to prevent the cascading effect of unprotected lay rescuers succumbing to gas exposures and amplifying the number of casualties. Studies of caves on other volcanic edifices or with potential gas hazards particularly at high altitudes would benefit from these considerations. A baseline now exists for hazardous cave atmospheres at Mount Rainier and repeat observations would be beneficial for volcano hazard monitoring.

ACKNOWLEDGEMENTS

Financial and equipment support from National Geographic Expeditions Council, the Mazamas Research Grant, the Mountain Rescue Association, Petzl, REI, Alberta Speleological Society, and National Speleological Society. Aaron Messinger and Special Projects Operations, supplier of SCBA equipment. Tom Gall, expedition HAZMAT specialist, John Panches, Tom Wood, safety officers, and Woody Peeples, Expedition Doctor. Additional cave surveyors 2015-2017, Tabbatha Cavendish, David Riggs, Nick Vieira, and Barb Williams. Cracker Jack First Response Specialists facilitated logistics for the 2015 field portion. John Meyers and Dave Clarke coordinated porter teams. Linda Sobolewski, Rick Davis, and Glyn Williams-Jones for helpful advice. The one hundred personnel who facilitated the studies by portering scientific and expedition equipment to the summit and back, supported by Corvallis Mountain Rescue (OR), Deschutes Mountain Rescue (OR), Everett Mountain Rescue (WA), Hood River Crag Rats (OR), Olympic Mountain Rescue (WA), Portland Mountain Rescue (OR), Volcano Rescue Team (WA), and the Douglas County Sheriff's Mountain Rescue Unit (OR). Research and collecting permit from the United States Department of the Interior- National Park Service – Mount Rainier. W.C. Evans and an additional reviewer provided comments which were very helpful to improving the manuscript. We thank F. De Ruydts and T. Wood for images in Figure 2; SPO, and T. Wood for images in Figure 3; A. Parness and D. Riggs for images in Figure 7; F. De Ruydts for images in Figure 10.

REFERENCES

- Agency for Toxic Substances and Disease Registry, n.d., Medical Management Guidelines for Sulfur Dioxide: <https://www.atsdr.cdc.gov/MMG/MMG.asp?id=249&tid=46> (Accessed August 28, 2020).
- Anderson, C., n.d., Deadly Fumaroles: https://web.archive.org/web/20110717005030/http://glaciercaves.com/html/mounth_1.HTM (Accessed September 18, 2020).
- ASTM International, 2019, Standard Practice for Respiratory Protection, F3387-19: ASTM International: West Conshohocken, PA, USA, 31 p.
- Avon Protection, n.d., FM53 the multiple mission mask: <https://www.avon-protection.com/products/fm53.htm> (Accessed August 28, 2020).
- Badino, G., 2009, The legend of carbon dioxide heaviness: *Journal of Cave and Karst Studies*, v. 71, no. 1, p. 100–107.
- Berberan-Santos, M., Bodunov, E., and Pogliani, L., 1997, On the barometric formula: *American Journal of Physics*, v. 65, no. 5, 404 <https://doi.org/10.1119/1.18555>
- Cantrell, L. and Young, M., 2009, Fatal fall into a volcanic fumarole: *Wilderness and Environmental Medicine*, v. 20, no.1, p. 77–79. <https://doi.org/10.1580/08-WEME-CR-199.1>
- Cartaya, E., 2018, Hybrid counterweight system for glacier fumarole rescue applications [abs.]: International Technical Rescue Symposium 2018, Portland, USA, 8 p.
- Centers for Disease Control and Prevention, 1994, Carbon dioxide immediately dangerous to life or health concentrations (IDLH): <https://www.cdc.gov/niosh/idlh/124389.html> (Accessed August 28, 2020).
- Centers for Disease Control and Prevention, 1994, Sulfur dioxide immediately Dangerous to life or health concentrations (IDLH). <https://www.cdc.gov/niosh/idlh/7446095.html> (Accessed August 28, 2020).
- Centers for Disease Control and Prevention, 1994, Hydrogen sulfide immediately dangerous to life or health concentrations (IDLH): <https://www.cdc.gov/niosh/idlh/7783064.html> (Accessed August 28, 2020).
- Coombs, H.A., 1936. The geology of Mount Rainier National Park: University of Washington Publications in Geology., v. 3, no. 2. University of Washington: Seattle, Washington, p. 202–203.
- Curtis, A., 2016, Dynamics and global relevance of fumarolic ice caves on Erebus Volcano, Antarctica [Ph.D. thesis]: Socorro, New Mexico Institute of Mining and Technology, https://aaroncurt.is/paper/curtis2016-phd_diss.pdf (Accessed August 28, 2020).
- Curtis, A., 2020, Comparison of Earth's fumarolic ice caves, with implications for icy voids on other worlds [abs.]: 3rd International Planetary Caves Conference, San Antonio, Texas. 1 p.
- D'Alessandro, W., 2006, Gas hazard: An often neglected natural risk in volcanic areas: *WIT Transactions on Ecology and the Environment*. <https://doi.org/10.2495/GEO060371>
- Davis, R., Anitori, R., Stenner, C., Smith, J., and Cartaya, E., 2020, Fumarolic glacial and firn ice caves on Mt. St. Helens may provide insight into Martian subsurface microbial communities [abs.]: Analog Field Sites Mini Symposium, Houston, Texas. The Lunar and Planetary Institute, Open University Astrobiology, and NASA Johnson Space Center.

- Enform, 2013, H₂S Alive: Hydrogen Sulfide Training: 7th Ed. Enform Canada; Calgary, Canada, 121 p.
- Ewert, J.W., Diefenbach, A.K., and Ramsey, D.W., 2018, 2018 update to the U.S. Geological Survey national volcanic threat assessment: U.S. Geological Survey Scientific Investigations Report 2018–5140, 40 p. <https://doi.org/10.3133/sir20185140>
- Florea, L., Pflitsch, A., Cartaya, E., and Stenner, C., 2021, Microclimates in fumarole ice caves on volcanic edifices-Mount Rainier, Washington, USA: *Journal of Geophysical Research, Atmospheres*. v. 126, no. 4, p. 1–15. <https://doi.org/10.1029/2020JD033565>
- Frank, D., 1995, Surficial extent and conceptual model of hydrothermal system at Mount Rainier: Washington. *Journal of Volcanology and Geothermal Research*, v. 65, no. 1, p. 51–80. [https://doi.org/10.1016/0377-0273\(94\)00081-Q](https://doi.org/10.1016/0377-0273(94)00081-Q)
- Hansell, A., and Oppenheimer, C., 2005, Health hazards from volcanic gases: A Systematic Literature Review: *Archives of Environmental Health: An International Journal*. v.59., no.12, p. 628–639. <https://doi.org/10.1080/00039890409602947>
- Illanko, T., Fischer, T., Kyle, P., Curtis, A., Lee, H., and Sano, Y., 2019, Modification of fumarolic gases by the ice-covered edifice of Erebus volcano, Antarctica: *Journal of Volcanology and Geothermal Research*. v. 381, p 119–139. <https://doi.org/10.1016/j.jvolgeores.2019.05.017>
- Ingraham, E.S., 1895. The pacific forest reserve and Mt. Rainier: The Calvert Company, Seattle, WA, p. 21–23.
- KGW Staff, 2014, Tualatin man in fair condition after Mt. Hood fall: KGW. <https://www.kgw.com/article/news/tualatin-man-in-fair-condition-after-mt-hood-fall/318116102> (Accessed September 14, 2020).
- Kiver, E. P., 1978, Mount Baker's changing fumaroles: *Ore Bin*, v. 40, p. 133–145.
- Kiver, E.P., and Mumma, M.D., 1971, Summit firn caves, Mount Rainier, Washington: *Science*, v. 173. pp. 320–322. <https://doi.org/10.1126/science.173.3994.320>.
- Kiver, E.P., and Steele, W.K., 1975, Firn caves in the volcanic craters of Mount Rainier: *The NSS Bulletin*. v. 37., no. 3. p. 45–55.
- Le Guern, F., Ponzevera, E., Lokey, W, and Schroedel, R.D., 2000, Mount Rainier summit caves volcanic activity: *Washington Geology*, v. 28, no. 1/2, p. 25.
- McKay, R., 2020, Respirator use at high altitudes: *The Synergist*, Jan, 2020. American Industrial Hygiene Association. <https://synergist.iah.org/202001-respirator-use-at-high-altitudes> (Accessed August 12, 2020).
- National Academies of Sciences, Engineering, and Medicine, 2019, *An astrobiology strategy for the search for life in the universe*: Washington, DC: The National Academies Press, 188 p. <https://doi.org/10.17226/25252>.
- National Park Service, 2020, Mount Rainier / Climbing: <https://www.nps.gov/mora/planyourvisit/climbing.htm> (Accessed August 18, 2020).
- National Research Council. 1994. Mount Rainier: Active cascade volcano: Washington, D.C.: The National Academies Press, 128 p. <https://doi.org/10.17226/4546>
- Nehring, N.L., Wollenberg, H.A., and Johnston, D. A., 1981, Gas analysis of fumaroles from Mt. Hood, Oregon: US Geological Survey Open File Report 81-236, 9 p.
- Ocenco, n.d., M-20 SCSR: <https://www.ocenco.com/> (Accessed August 16, 2020).
- Owen, T., Biemann, K., Rushneck, D.R., Biller, J.E., Howarth, D.W., and Lafleur, A.L., 1977, The composition of the atmosphere at the surface of Mar.: *Journal of Geophysical Research*. v. 82, no. 28. P. 4635–4639. <https://doi.org/10.1029/JS082i028p04635>.
- Pflitsch, A., Cartaya, E., McGregor, B., Holmgren, D., and Steinhöfel, B., 2017, Climatologic studies inside Sandy Glacier at Mount Hood Volcano in Oregon, USA: *Journal of Cave and Karst Studies*, v. 79, no. 3, p. 189–206. <http://dx.doi.org/10.4311/2015IC0135>.
- Rom, W., 1992, *Environmental and Occupational Medicine*: 2nd ed; Little, Brown; Boston, 1493 p.
- Savitzky, A., and Golay, M., (1964). Smoothing and differentiation of data by simplified least squares procedures: *Analytical Chemistry* v. 36, no.8, p. 1627–1639. doi:10.1021/ac60214a047.
- Sobolewski, L., Stenner, C., Hüser, C., Berghaus, T., Cartaya, E., and Pflitsch, A., 2020. Formation and evolution of newly formed glaciovolcanic caves in the crater of Mount St. Helens, Washington, USA: *The Cryosphere Discussions*. <https://doi.org/10.5194/tc-2020-279>.
- Special Projects Operations, 2015, ELABS – Extreme Limited Access Breathing System: <https://dwe-spo.com/shop/elabs/> (Accessed August 28, 2020).
- Spelce, D.L., McKay, R.T. Johnson, J.S., Rehak, T.R., and Metzler, R.W., 2016, Respiratory protection for oxygen deficient atmospheres: *Journal of the International Society of Respiratory Protection*. v. 33, no. 2, PMID: 32336876; PMCID: PMC7183576.
- Spelce, D.L., Metzler, R.W., Johnson, J.S., Rehak, T.R., and McKay, R.T., 2017, Revisiting respirators for Oxygen-deficient atmospheres: A comparison of OSHA and Z88.2 approaches to respiratory protection: *The Synergist*, March 2017. <https://synergist.iah.org/201703-revisiting-respirators-for-o2-deficiency> (Accessed August 12, 2020).
- Stevens, H., 1876. The ascent of Mount Tahoma: *Atlantic Monthly*. Nov., p. 511–530.
- Stix, J., and de Moor, J.M., 2018, Understanding and forecasting phreatic eruptions driven by magmatic degassing: *Earth Planets Space*, v. 70, no. 83. <https://doi.org/10.1186/s40623-018-0855-z>
- Tebo, B. M., Davis, R. E., Anitori, R. P., Connell, L. B., Schiffman, P., and Staudigel, H., 2015, Microbial communities in dark oligotrophic volcanic ice cave ecosystems of Mt. Erebus, Antarctica: *Frontiers in Microbiology*, v. 6, no. 179. <https://doi.org/10.3389/fmicb.2015.00179>.
- Tomlinson, S., 2019, Mount Hood rescuers develop new protocols to save fallen climbers from toxic volcanic vents: *The Oregonian*. https://www.oregonlive.com/pacific-northwest-news/2015/04/fumaroles_mount_hood_rescuers.html (Accessed September 18, 2020).
- Williams-Jones, G. and Rymer, H., 2015, Hazards of volcanic gases: *in* Sigurdsson, H., Houghton, B. McNutt, S., Rymer, H., Stix, J., eds., *The Encyclopedia of Volcanoes*. 2nd ed. Academic Press, p. 985–992, <https://doi.org/10.1016/B978-0-12-385938-9.00057-2>.
- Young, M., 2015, Mt. Hood rescuers reach 3 climbers, including 2 who are injured, after fall: https://www.oregonlive.com/clackamascounty/2015/01/mt_hood_rescue.html (Accessed September 18, 2020).
- Zimelman, D. R., Rye, R. O., and Landis, G. P., 2000, Fumaroles in ice caves on the summit of Mount Rainier—preliminary stable isotope, gas, and geochemical studies: *Journal of Volcanology and Geothermal Research*, v. 97, p. 457–473, [https://doi.org/10.1016/S0377-0273\(99\)00180-8](https://doi.org/10.1016/S0377-0273(99)00180-8).